J|A|C|S
ARTICLES

Published on Web 11/30/2010

Theoretical Elucidation of the Competitive Electro-oxidation Mechanisms of Formic Acid on Pt(111)

Wang Gao, John A. Keith, Josef Anton, and Timo Jacob*

Institut für Elektrochemie, Universität Ulm, Albert-Einstein-Allee 47, D-89081 Ulm, Germany

Received September 25, 2010; E-mail: timo.jacob@uni-ulm.de

Abstract: The mechanisms of formic acid (HCOOH) oxidation on Pt(111) under electrochemical conditions have been studied using density functional theory and then compared with the analogous gas-phase reaction. Results show that HCOOH oxidation under a water-covered surface behaves substantially differently than in the gas phase or using a solvation model involving only a few water molecules. Using these models, we evaluated the detailed reaction process, including energies and geometric structures of intermediates and transition states under the influence of different solvation models and electrode potentials. Our calculations indicate that this potential-dependent electrochemical oxidation proceeds via a multipath mechanism (involving both the adsorbed HCOOH and HCOO intermediates), a result succinctly rationalizing conflicting experimental observations. Moreover, this study highlights how subtle changes in electrochemical reaction environments can influence (electro)catalysis.

Introduction

The electro-oxidation of formic acid (HCOOH) on Pt-group metals has attracted great interest over the past decades because of its status as a fundamental electrochemical oxidation reaction as well as its relevance in low-temperature fuel cells.[1−21] It is generally accepted that electrochemical oxidation of HCOOH on platinum proceeds via a dual-path mechanism consisting of *indirect* and *direct* pathways. The indirect path has HCOOH converting first to adsorbed CO and then to CO_2. In contrast, the direct path reacts to CO_2, but through which intermediate (if any) the mechanism runs has been debated.

Numerous experimental studies have presented different perspectives on what may be the relevant intermediates in HCOOH oxidation. *In situ* infrared reflection−absorption spectroscopy (IRAS) experiments identified adsorbed CO, a product of HCOOH dehydration, as a poisonous species, evidencing the indirect path.[4,7] Both Osawa et al.[14−18] and Behm et al.[18−21] have reported polycrystalline surfaces covered with adsorbed CO at potentials below 0.3 V vs the reversible hydrogen electrode (RHE), decreasing CO coupled with increasing formate (HCOO) concentrations between 0.3 and 0.7 V, and then surfaces primarily covered with HCOO above 0.9 V.

It is the identity of the reactive intermediate in the direct path that is particularly controversial. Wilhelm and co-workers initially believed that either COH or CHO would be the reactive intermediate,[5] while others have long assumed it is COOH.[3,8,9] Recently, IR spectroscopy studies by Osawa et al. indicated that HCOO is the reactive intermediate and that oxidation of HCOO to CO_2 is rate-determining.[14−16] In contrast, using the same IR techniques, studies by Behm et al. indicated HCOO to *not* be the reactive intermediate but a spectator, and weakly adsorbed HCOOH could then be the intermediate in the dominant reaction path.[19−21] Finally, formic oxidation experiments at elevated temperatures lead to increased currents but decreased concentrations of formate, suggesting either that formate formation is slower than formate decomposition or that the formate pathway is not dominant.[18]

Given these observations, Behm et al.[19−21] have proposed that the formic acid oxidation mechanism should be considered as at least three different pathways, each starting from adsorbed formic acid (Scheme 1). The *indirect pathway* operates via a CO intermediate, which is a product of dehydrogenation of formic acid. The *direct pathway* likely operates via a weakly

(1) Breiter, M. W. *J. Electroanal. Chem.* **1967**, *14*, 407–413.
(2) Capon, A.; Parson, R. *J. Electroanal. Chem.* **1973**, *44*, 1–7.
(3) Capon, A.; Parsons, R. *J. Electroanal. Chem.* **1973**, *45*, 205–231.
(4) Kunimatsu, K.; Kita, H. *J. Electroanal. Chem.* **1987**, *218*, 155–172.
(5) Wilhelm, S.; Vielstich, W.; Buschmann, H.; Iwasita, T. *J. Electroanal. Chem.* **1987**, *229*, 377–384.
(6) Parsons, R.; VanderNoot, T. *J. Electroanal. Chem.* **1988**, *257*, 9–45.
(7) Corrigan, D. S.; Weaver, M. J. *J. Electroanal. Chem.* **1988**, *241*, 143–162.
(8) Sun, S.; Clavilier, J.; Bewick, A. *J. Electroanal. Chem.* **1988**, *240*, 147–159.
(9) Lamy, C.; Leger, J. M. *J. Chim. Phys. Phys.-Chim. Biol.* **1991**, *88*, 1649.
(10) Kizhakevariam, N.; Weaver, M. J. *Surf. Sci.* **1994**, *310*, 183–197.
(11) Marković, N. M.; Gasteiger, H. A.; Ross, P. N.; Jiang, X.; Villegas, I.; Weaver, M. J. *Electrochim. Acta* **1995**, *40*, 91–98.
(12) Jarvi, T. D.; Stuve, E. M. In *Electrocatalysis*; Lipkowski, J., Ross, P., Eds.; Wiley-VCH: Weinheim, 1998; pp 75−153.
(13) Rice, C.; Ha, S.; Masel, R. I.; Wieckowski, A. *J. Power Sources* **2003**, *115*, 229–235.
(14) Samjeské, G.; Osawa, M. *Angew. Chem., Int. Ed.* **2005**, *44*, 5694–5698.
(15) Samjeské, G.; Miki, A.; Ye, S.; Yamakata, A.; Mukouyama, Y.; Okamoto, H.; Osawa, M. *J. Phys. Chem. B* **2005**, *109*, 23509–23516.
(16) Mukouyama, Y.; Kikuchi, M.; Samjeské, G.; Osawa, M.; Okamoto, H. *J. Phys. Chem. B* **2006**, *110*, 11912–11917.
(17) Samjeské, G.; Miki, A.; Ye, S.; Osawa, M. *J. Phys. Chem. B* **2006**, *110*, 16559–16566.
(18) Chen, Y. X.; Ye, S.; Heinen, M.; Jusys, Z.; Osawa, M.; Behm, R. J. *J. Phys. Chem. B* **2006**, *110*, 9534–9544.
(19) Chen, Y. X.; Heinen, M.; Jusys, Z.; Behm, R. J. *Angew. Chem., Int. Ed.* **2006**, *45*, 981–985.
(20) Chen, Y.; Heinen, M.; Jusys, Z.; Behm, R. J. *Langmuir* **2006**, *22*, 10399–10408.
(21) Chen, Y.; Heinen, M.; Jusys, Z.; Behm, R. J. *ChemPhysChem* **2007**, *8*, 380–385.

Scheme 1. Mechanistic Scheme for Electrochemical Formic Acid Oxidation

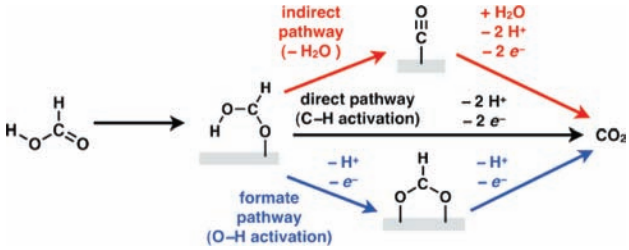

bound HCOOH intermediate and is initiated by C−H bond activation. The *formate pathway* operates via a HCOO intermediate and is initiated by O−H bond activation.

First-principles simulations should help clarify these conflicting experimental studies. Unfortunately, few theoretical studies exist on HCOOH oxidation on the Pt/H_2O system since modeling interactions between formic acid and water, especially at solid/liquid interfaces, is quite challenging. Nevertheless, some first-principles simulations on the well-defined Pt(111) surface in the presence of solution and applied potentials have been applied to investigate HCOOH oxidation.

Notably, computational results obtained by Neurock et al.[22] showed that COOH might be the reactive intermediate while HCOO is just a spectator, thereby showing the direct pathway is active, supporting experiments by Behm et al. Neurock et al. also found that an applied potential has little effect on the barriers of formate oxidation, but applied potentials significantly influence CO oxidation. Although these results appear to support some experiments, they are based on an adsorbed HCOOH* model that several independent theoretical investigations have reported as energetically less favorable.[23−25] Wang and Liu have used continuum solvation approaches to model the Pt/H_2O interface, finding that a weakly adsorbed HCOOH* with its CH bond in a "down" configuration is the reactive intermediate.[26] Their results also suggested that applied potentials have minor effects on HCOOH oxidation barriers.

Solvation typically plays a critical role in electrocatalysis. What that role is in HCOOH oxidation has not yet been addressed. To elucidate the controversial mechanism and investigate how different explicit water models affect these mechanisms, we studied HCOOH oxidation with density functional theory (DFT) in a simulation designed to model an electrochemical interface. We used two different explicit solvation models to simulate the aqueous interface, which we believed would play an important role in HCOOH oxidation. A large number of unique reaction pathways involving subtly different reaction intermediates and transition states were explicitly obtained. Effects of applied potentials were later included to investigate different preferred electrocatalytic pathways. By comparison to analogous simulations in the gas phase, our results can clarify the critical role of explicit water molecules on HCOOH oxidation and further clarify this complicated fundamental electrocatalytic mechanism.

Methods

All calculations were performed using the CASTEP code[27] with Vanderbilt-type ultrasoft pseudopotentials[28] and the generalized gradient approximation (GGA) exchange-correlation functional proposed by Perdew, Burke, and Ernzerhof (PBE).[29] Our simulations used one reacting HCOOH molecule on the $p(3\times3)$ Pt(111) surface unit cell. This model corresponds to an adsorbate surface coverage of 1/9 ML. In a previous work we investigated different surface coverages.[25] A five-layered slab represented the Pt(111) surface, and a vacuum width >13 Å minimized interactions between neighboring slabs in the supercell geometry. For each slab, the topmost three surface layers were allowed to relax, while the bottom two layers were fixed to the calculated crystal structure. Integrations in reciprocal space used a 2×2 Monkhorst−Pack k-point grid after test calculations with the 4×4 k-point grid amounted to energy differences <0.04 eV. A plane-wave basis set with an energy cutoff of 400 eV was used in all calculations. To investigate the reaction pathways, the transition state (TS) search procedure in the CASTEP code was used, which employs a combination of LST/QST (linear and quadratic synchronous transit, see ref 30 for details) algorithms with subsequent conjugate gradient methods.[27]

We define the binding energy (i.e., the adsorption energy) E_{bind} for co-adsorbed H_2O and HCOOH on Pt(111) as

$$E_{bind} = -(E_{total} - E_{surf} - E_{HCOOH} - nE_{H_2O}) \qquad (1)$$

where E_{total} is the energy of a H_2O/HCOOH cluster on Pt(111), E_{surf} is the energy of the clean Pt(111), E_{HCOOH} is the energy of an HCOOH molecule in vacuum, and nE_{H_2O} is the energy of a single H_2O molecule in a vacuum times the number of water molecules in the simulation box, n. All other adsorption energies are defined in a similar way. Applied electrode potentials are incorporated by explicitly shifting Fermi energies as calculated by DFT. More details of this approach can be found in ref 31.

Results and Discussion

To distinguish between the different calculated reaction processes, we discuss various pathways based on different solvation models (labeled **A** and **B**). In model **A**, we used two explicit water molecules per surface unit cell to describe the interfacial waters. In model **B**, a water bilayer consisting of a fully periodic ice-like network of water molecules was used to describe the solid/liquid interface.

The modeled reaction pathways are summarized in Scheme 2. Using these models, we obtained two different structures for HCOOH* (labeled **1** and **2**) that are the starting point for each subsequent mechanism. As electrocatalytic processes may occur via either Langmuir−Hinshelwood (LH)-type pathways (where all reacting intermediates are on the surface) or Eley−Rideal (ER)-type reactions (where the electrolyte plays an explict role in protonation reactions), we consider both.

HCOOH* Adsorption Structures. Using solvation model **A**, two different configurations of HCOOH and water are possible. The unique structures have nearly the same overall binding

(22) Neurock, M.; Janik, M.; Wieckowski, A. *Faraday Discuss.* **2008**, *140*, 363–378.
(23) Bakó, I.; Pálinkás, G. *Surf. Sci.* **2006**, *600*, 3809–3814.
(24) Hartnig, C.; Grimminger, J.; Spohr, E. *J. Electroanal. Chem.* **2007**, *607*, 133–139.
(25) Gao, W.; Keith, J. A.; Anton, J.; Jacob, T. *Dalton Trans.* **2010**, *39*, 8450–8456.
(26) Wang, H.; Liu, Z. *J. Phys. Chem. C* **2009**, *113*, 17502–17508.
(27) Segall, M. D.; Lindan, P. J. D.; Probert, M. J.; Pickard, C. J.; Hasnip, P.; Clark, S. J.; Payne, M. *J. Phys.: Condens. Matter* **2002**, *14*, 2717–2744.
(28) Vanderbilt, D. *Phys. Rev. B* **1990**, *41*, 7892–7895.
(29) Perdew, J. P.; Burke, K.; Ernzerhof, M. *Phys. Rev. Lett.* **1996**, *77*, 3865–3868.
(30) Govind, N.; Petersen, M.; Fitzgerald, G.; King-Smith, D.; Andzelm, *J. Comp. Mater. Sci.* **2003**, *28*, 250–258.
(31) Keith, J. A.; Jerkiewicz, G.; Jacob, T. *ChemPhysChem* **2010**, *11*, 2779–2794.

Scheme 2. Formic Acid Oxidation Mechanisms[a]

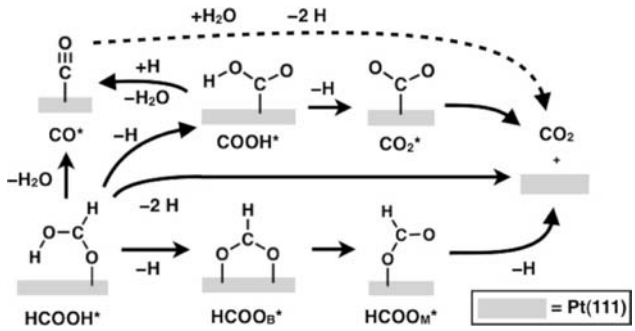

[a] Solid arrows denote mechanisms reported in this work.

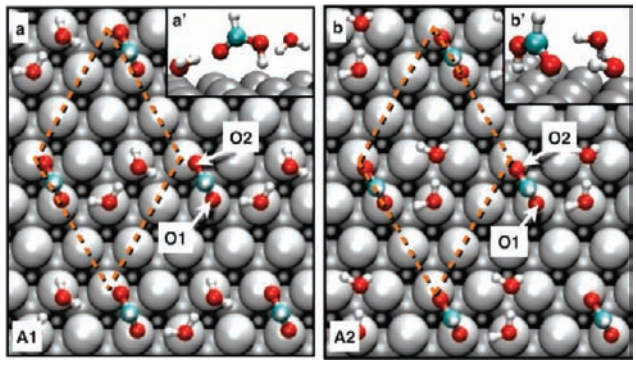

Figure 1. (a) **A1** and (b) **A2** HCOOH structures with two waters on Pt(111). Insets (a′,b′) denote side views of the interface.

energies: **A1** (Figure 1a) has $E_{bind} = 1.24$ eV, while **A2** (Figure 1b) has $E_{bind} = 1.27$ eV. In both cases, HCOOH* binds with its carbonyl oxygen (O1) to an atop site and its OH group (O2) pointing *down* toward another adjacent atop site, but the water molecules are aligned slightly differently.

In previous calculations[25] we found that a single water molecule within a (3×3) unit cell ($\theta = 1/9$ ML) binds to the surface by 0.33 eV, while a single HCOOH binds to this surface with a binding energy of 0.40 eV. The binding energy of HCOOH* + H_2O on this surface was found to be the same as the sum of these two energies (0.73 eV), showing that at this low coverage a single water molecule hardly affects HCOOH* binding to the surface. Thus, as a first approximation, one might have expected the total binding energy of HCOOH* + $2H_2O$ in both **A1** and **A2** models to be the sum of E_{bind} of HCOOH*, two water molecules, and an H-bond between the waters (∼0.2 eV). Indeed, this simple approximation is confirmed by our calculations.

Table 1 shows geometric details for HCOOH within the explicit solvation models. The different orientations of waters between **A1** and **A2** affect the H-bond between water molecules. In **A1**, we find an increased bond angle θ_{HOH} of the first water to be 110.36° but a normal bond angle of 104.65° in **A2**. Notably, the HCOOH molecules in both **A1** and **A2** are aligned perpendicular to the surface.[25] The O1−Pt and O1−H H-bond distances in **A1** and **A2** show that **A1** binds more strongly to other surface adsorbates (in this case water), while **A2** binds more strongly to the Pt surface. The similarity in binding energies for these species indicates, however, that neither configuration of water molecules is strongly preferred over the other.

The full bilayer in model **B** causes all H-bonds to be well-defined, eliminating ambiguity regarding H-bond positions found

Table 1. Geometric Data for Different HCOOH Structures on the (3×3) Pt(111) Surface Unit Cell[a]

adsorbate	d_{O1-Pt}	d_{O2-Pt}	d_{O1-H}	d_{O2-H}	d_{Pt-H_2O}	$\theta^1_{H_2O}$	$\theta^2_{H_2O}$
HCOOH + H_2O	2.24	3.13	1.79		2.09	106.7	
A1	2.70	3.18	1.74		2.19	110.4	
A2	2.52	3.15	1.84		2.22	104.7	
B1	3.55	2.93	1.97	2.05		102.7	107.9
B2	3.87	3.68	1.86	1.99		108.8	101.6

[a] HCOOH + H_2O denotes structural information for HCOOH solvated by a single water molecule. Structures **A1** and **A2** are models for HCOOH solvated with two waters, while structures **B1** and **B2** show HCOOH solvated with a water bilayer. The CO oxygen in HCOOH is denoted O1, while the OH-group oxygen is denoted O2. d_{O1-H} and d_{O2-H} are the H-bond lengths between HCOOH and the adjacent water molecule. d_{Pt-H_2O} denotes the distance between the water molecule adjacent to O1 and the nearest Pt atom. $\theta^1_{H_2O}$ and $\theta^2_{H_2O}$ are the intramolecular bond angles of waters coordinating to O1 and O2, respectively. Distances in Å and angles in degrees.

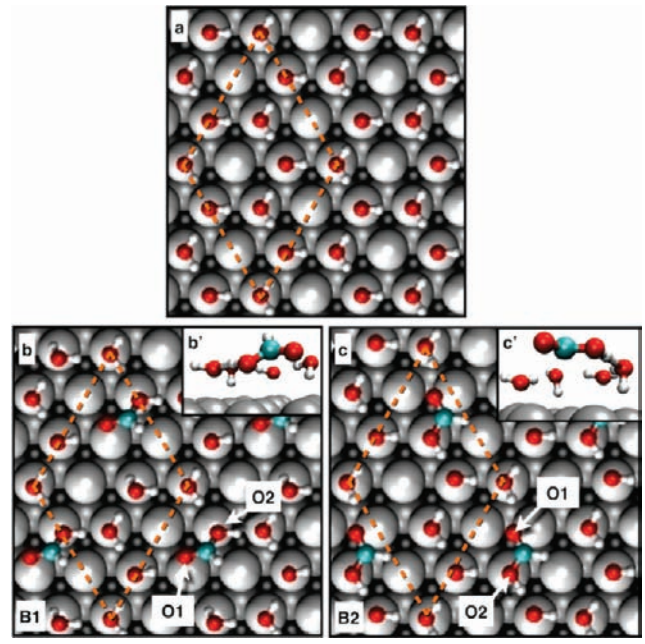

Figure 2. (a) Top view of the water bilayer structure on Pt(111). (b) **B1** and (c) **B2** HCOOH structures with four waters on Pt(111). Insets (b′,c′) denote side views of the interface.

with model **A**. Nevertheless, two unique structures were also found with model **B**. Figure 2a depicts waters in the ordered ice-like structure where the outer waters have their OH bonds pointing toward the surface.[32] When HCOOH is incorporated into this surface, its size and structure permits it to substitute two water molecules in the bilayer. An HCOOH/H_2O cluster thereby forms with two neighboring H_2O molecules, all of which fits in the H-bonding network spanning the entire unit cell.

With this observation, we found two stable ring-network structures dependent on the direction of HCOOH, both with similar binding energies: $E_{bind} = 2.48$ eV (**B1**, Figure 2b) and 2.60 eV (**B2**, Figure 2c). In **B1**, the O−H bond in HCOOH forms an H-bond with a water molecule that lies parallel to Pt(111). In **B2**, the O−H also forms a H-bond, but with a water oriented perpendicularly to Pt(111). Based on observed atomic distances tabulated in Table 1, HCOOH in **B1** interacts more strongly with the Pt surface, while HCOOH in **B2** interacts more strongly with co-adsorbates. As a result, HCOOH in **B2**

(32) Jacob, T.; Goddard, W. A. *J. Am. Chem. Soc.* **2004**, *126*, 9360–9368.

practically lies flat on the surface to maximize the number of H-bonds to adjacent water molecules. Wang and Liu reported a different structure for HCOOH, whereby HCOOH binds with four H_2O molecules and adsorbs on the surface with its CH bond pointing toward the surface.[26] Direct comparison to that work is not possible, but in our own calculations, the C−H down structure is >0.6 eV less stable (E_{bind} = 1.84 eV) than either structure we calculated in our models **B1** and **B2**.

Oxidation Pathways Not Involving CO Intermediates. A. CO_2 Formation by Simultaneous C−H and O−H Activation. Using solvation model **A**, the direct pathway involving simultaneous C−H and O−H activation from HCOOH* to CO_2 has very large barriers (**A1**, E_{act} = 3.01 eV; **A2**, E_{act} = 2.45 eV). Both barriers are higher than the barrier of the system with a single water (E_{act} = 2.12 eV).[25] Using solvation model **B**, the barriers are somewhat lower (**B1**, E_{act} = 1.68 eV; **B2**, E_{act} = 1.43 eV), indicating that the water bilayer catalyzes this process. Despite this catalytic effect, the barriers remain relatively high, and this will be later ruled out as a possible reaction process on Pt(111) terraces.

B. CO_2 Formation Initiated by C−H Activation. Starting from HCOOH*, C−H activation can lead to COOH*. Again, different initial structures lead to different transition states, which finally result in different product structures. In the **A1** and **A2** models, this process is exothermic by −0.52 and −0.32 eV, respectively. The respective process barriers are 1.68 and 1.67 eV. In comparison, these barriers are reasonably close to the C−H activation barrier for HCOOH* oxidation in the gas phase on a low-coverage (3×3) unit cell (E_{act} = 1.83 eV), but this barrier is much lower than that found in gas phase with a higher coverage (2×2) unit cell (E_{act} = 4.30 eV).[25] Again, coverage effects play a large role in these calculated barrier heights, but the presence of a second water does not further reduce the C−H activation barrier substantially.

In **B1** and **B2** models, C−H activation from HCOOH* leads to two different products as well. In the **B1** model, C−H activation leads to a spontaneous O−H bond-breaking step, which then leads to an adsorbed CO_2* intermediate. This intermediate will be discussed in more detail below. Interestingly, other calculations on O−H bond activation from COOH* into an aqueous phase indicate that this is a barrier-less process.[22,33−35] The concerted reaction step from the **B1** structure is overall exothermic by −0.33 eV and has a barrier of E_{act} = 0.79 eV. In the **B2** model, O−H bond-breaking does not accompany C−H bond-breaking, and so COOH* is formed instead. Here, the reaction step is slightly endothermic by +0.07 eV and has a barrier of E_{act} = 1.63 eV.

Of the four different calculated pathways, the **B1** pathway is the lowest and also permits simultaneous C−H and O−H bond activation. This particular reactivity is most likely due to a combination of two things. First, the water bilayer in the **B1** model promotes O−H bond dissociation. Second, the **B1** model has HCOOH* binding more strongly to the surface, so CO_2* can remain bound. In previous calculations by Neurock et al. on the upright HCOOH*, C−H activation came with a barrier of 0.50 eV.[22] A similar barrier of E_{act} = 0.45 eV was proposed in the CH-down configuration by Wang and Liu.[26] In comparison, our **B1** reaction barriers is slightly higher, probably because we initiated our studies with a more stable HCOOH* configuration.

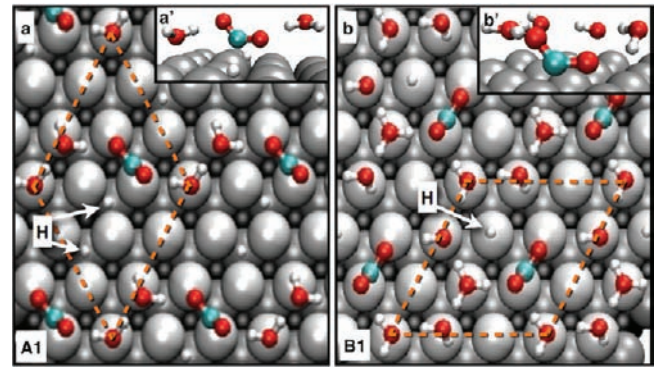

Figure 3. (a) Top view of the CO_2* intermediate structure on Pt(111) with model **A1** involving two explicit water molecules. (b) Top view of the CO_2* intermediate structure on Pt(111) with model **B1** involving four water molecules in a bilayer structure. Insets (a′,b′) denote side views of the interface.

Although the **B1** pathway leads directly to CO_2*, O−H activation from COOH* in the **A1**, **A2**, and **B2** models must still occur for oxidation to proceed. COOH* binds to the surface via a Pt−C bond in these structures. For **A1**, after O−H activation, another adsorbed CO_2* intermediate is found, analogous to that seen in the **B1** pathway. (The CO_2* intermediates will be discussed shortly.) This O−H activation step is endothermic by +0.31 eV and has a barrier of E_{act} = 1.40 eV. O−H activation from the less stable COOH* structure in the **A2** model is isoenergetic, with a lower barrier of E_{act} = 1.05 eV. In the **B2** model, the reaction is also essentially isoenergetic, but with a substantially lower barrier of only E_{act} = 0.48 eV.

The CO_2* intermediate encountered in the **A1** and **B1** models deserves special mention (Figure 3). In both cases, a H-bond network due to explicit waters stabilizes the CO_2* intermediate. The CO_2* intermediate is metastable in that it is −0.21 and −0.33 eV more stable than the preceding HCOOH* intermediate in the **A1** and **B1** models, respectively. This means that, under specific configurations of water molecules, highly stable molecules such as CO_2 can be confined close to a surface with van der Waals interactions, as has been seen with organic molecular porous materials.[36] Naturally, these CO_2* intermediates on Pt(111) are expected to be short-lived, however. For **A1**, desorption of CO_2* is exothermic by −0.17 eV, with a small barrier of 0.21 eV. For **B1**, the process is essentially isoenergetic, but the water bilayer gives less lateral room for release of CO_2, so the barrier is slightly higher: 0.48 eV.

Comparing calculations from models **A** to those from models **B**, one easily sees the importance of the water bilayer in describing O−H activation steps. Without the extensive H-bonding network due to the bilayer, barriers for O−H bond-breaking can be more than 2 times greater than without the catalytic effects from nearby waters. Furthermore, the different orientations of the HCOOH* and COOH* can lead to different pathways. Coincidentally, both the **A1** and **B1** models have a CO_2* intermediate, while the **A2** and **B2** models react to form a CO_2 molecule that does not interact with the surface. Overall, the most relevant pathway to be considered for all the direct mechanisms, however, is that with the lowest energy: the **B1** pathway.

C. CO_2 Formation via the Formate Intermediate. The formate pathway is initiated by O−H activation of the HCOOH* species. For the **A1** structure, O−H bond activation is practically isoenergetic, with an activation barrier of E_{act} = 0.63 eV. For the **A2** structure, the reaction is endothermic by 0.29 eV, with

(33) Gao, W.; Zhao, M.; Jiang, Q. *ChemPhysChem* **2008**, *9*, 2092–2098.
(34) Gong, X.; Hu, P.; Raval, R. *J. Chem. Phys.* **2003**, *119*, 6324.
(35) Spendelow, J. S.; Goodpaster, J. D.; Kenis, P. J. A.; Wieckowski, A. *J. Phys. Chem. B* **2006**, *110*, 9545–9555.

an activation barrier of $E_{act} = 0.75$ eV. Both barriers are larger than the O−H bond activation energy for HCOOH with single water: $E_{act} = 0.46$ eV.[25] The resulting HCOO intermediate, bound with a bidentate configuration ($HCOO_B$*), is adsorbed with two Pt−O bonds. The resulting $HCOO_B$* intermediate is adsorbed at a bridge site, where the O−Pt bond lengths are $L_{O1-Pt} = 2.19$ and $L_{O2-Pt} = 2.76$ Å in the **A1** model, and $L_{O1-Pt} = 2.18$ and $L_{O2-Pt} = 2.48$ Å in the **A2** model.

Using the solvation model **B**, similar $HCOO_B$* intermediates are found, but the calculated energies differ from those in model **A**. For the **B1** structure, O−H bond activation is exothermic by −0.31 eV, with a barrier of 0.29 eV, and both values are ∼0.3 eV less than those found with **A1** and **A2** models. For the **B2** structure, this reaction is endothermic by 0.24 eV but has a barrier of $E_{act} = 0.49$ eV. As both **B1** and **B2** models show lower energy products with lower reaction barriers, the water bilayer clearly plays a significant role with O−H activation barriers. The structural geometries of $HCOO_B$* clearly show substantially stronger bonding within the **B1** model: $L_{O1-Pt} = L_{O2-Pt} = 2.24$ Å in the **B1** model, and $L_{O1-Pt} = 2.24$ and $L_{O2-Pt} = 2.67$ Å in the **B2** model.

From these intermediates, $HCOO_B$* can react directly to form CO_2. For the **A1** structure, the reaction is exothermic by −0.35 eV, but the barrier (2.59 eV) is quite high since the H-bond network made by the two water molecules is now broken. For the **A2** structure, the reaction is exothermic by −0.62 eV, and the barrier is lower ($E_{act} = 1.40$ eV), partly due to the stabilization of the two waters, which had not been forming an expansive H-bond network. The smaller barrier is in reasonable agreement with previous calculations which found barriers in a range of 1.10−1.20 eV using different solvation models.[22,26]

In model **A**, the orientation of individual water molecules was found to play a significant role in the CO_2 formation. In model **B**, both systems facilitate CO_2 formation, giving barriers similar to the **A2** model. For $HCOO_B$* reacting to CO_2, the **B1** model's reaction is −0.26 eV exothermic, with a barrier of 1.63 eV, while the **B2** model's reaction is −0.19 eV exothermic, with a barrier of 1.46 eV. As **B1** and **B2** have different structures embedded in the water bilayer, the calculated values are slightly different, but not substantially.

An alternative route to form CO_2 is possible if the bidentate $HCOO_B$* rearranges to a monodentate $HCOO_M$* by breaking an O−Pt bond. As expected, all models find that the monodentate $HCOO_M$* intermediate is less stable than the bidentate $HCOO_B$* intermediate. For **A1**, the reaction is +0.33 eV endothermic, with a barrier of 0.65 eV. For **A2**, the reaction is +0.10 eV endothermic, with a barrier of 0.43 eV. The **A1** values are almost the same as those obtained with previous calculations on the gas-phase reaction with one water (endothermic by 0.32 eV, with a barrier of 0.69 eV).[25] For **B1**, the reaction is 0.58 eV endothermic, with a barrier of 0.61 eV. Finally, for **B2**, the reaction is 0.26 eV endothermic, with a barrier of 0.91 eV.

$HCOO_M$* must then break its C−H bond to form CO_2. C−H activation of $HCOO_M$* with the **A1** and **A2** models is exothermic by −0.69 and −0.72 eV, respectively, while the respective barriers are $E_{act} = 1.12$ and 1.18 eV. In the earlier model in the gas phase with one water molecule, the reaction was exothermic by −0.68 eV, with a barrier of $E_{act} = 0.92$ eV.[25] The second waters in solvation models **A** evidently only have a minor effect on the barriers, most likely due to crowding between water molecules at the interface during the transition state.

In contrast, the final C−H activation steps with the **B1** and **B2** models are exothermic by −0.85 and −0.46 eV, respectively, with activation barriers $E_{act} = 0.58$ and 1.10 eV. In general, the **B2** calculations match fairly well with the model **A** calculations, although the final CO_2 molecule is even less stable when sharing the interface with additional water molecules. In **B1** calculations, the orientation of $HCOO_M$* within the bilayer facilitates both easier C−H bond breaking and more-favorable bonding with CO_2 at the interface.

Overall, the reaction pathways with the lowest energy barriers are the most important in defining a reaction mechanism. Using solvation model **A**, the two lowest energy pathways calculated so far are the formate pathways operating through the $HCOO_M$* intermediate calculated in models **A1** and **A2**. Using solvation model **B**, the two lowest energy pathways are both found with system **B1**, and the reactions are the formate pathway operating through the $HCOO_M$* intermediate and the pathway leading to CO_2 via the CO_2* intermediate.

Pathways Involving CO Intermediates. In the indirect pathway, HCOOH* first decomposes to CO* and then further oxidizes to CO_2. This process was calculated to be exothermic with all solvation models. For models **A1**, **A2**, **B1**, and **B2**, the reactions are exothermic by −0.63, −1.05, −0.43, and −0.44 eV, respectively. In earlier calculations using only one water molecule, the reaction was −1.31 eV exothermic.[25] The highly varied energies show that minor differences in the structure of water at the surface can lead to very large changes in the CO* intermediate energies, but this can sometimes be adequately captured with solvation models involving only two water molecules (as in the case of model **A1**). The similarity in CO* energies implies that CO* bonding is less affected by orientation effects with the water bilayer, so the bilayer is perhaps a more consistent model for CO* at an electrochemical interface.

Although dehydrogenation of HCOOH* is calculated to be exothermic by all solvation models, all dehydrogenation barriers are very high. Calculations using models **A1**, **A2**, **B1**, and **B2** have barriers of $E_{act} = 3.34$, 3.21, 3.32, and 3.47 eV, respectively. Comparing these values to the calculated barrier with a single water molecule ($E_{act} = 3.74$ eV),[25] the presence of additional waters only somewhat lowers dehydrogenation barriers, but not by nearly enough to promote CO* formation. This means these indirect processes should not be considered competitive with the earlier discussed direct and formate pathways on terraces.

It is possible, however, that COOH* could dehydrogenate to form CO*. Since COOH* was not stable within the **B1** model, the barriers to form CO* in this mechanism from the **A1**, **A2**, and **B2** models are $E_{act} = 1.90$, 1.80, and 2.28 eV, respectively. All values are substantially lower than that in the system with a single water, $E_{act} = 2.74$ eV,[25] but again not low enough to be considered a competitive process compared to the other direct and formate pathways.

On the basis of these calculations alone, it would appear that CO* should not be formed in HCOOH oxidation at all. However, the presence of CO* is of course well established to be found on Pt(111) electrodes, particularly at relatively low applied potentials. Feliu and co-workers have shown that the presence of CO* seems to be proportional to the amount of step-edges and other defect sites on Pt(111).[37] Since our results show that dehydrogenation processes leading to CO* are always high-barrier processes on idealized Pt(111) terraces, our results

(36) Kim, H.; Kim, Y.; Yoon, M.; Lim, S.; Park, S. M.; Seo, G.; Kim, K. *J. Am. Chem. Soc.* **2010**, *132*, 12200–12202.
(37) Maciá, M. D.; Herrero, E.; Feliu, J. M. *Electrochim. Acta* **2002**, *47*, 3653–3661.

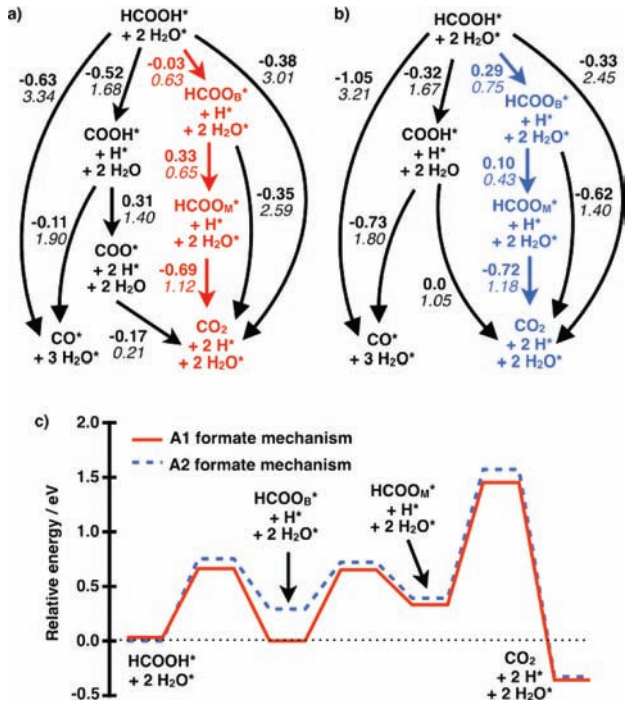

Figure 4. Langmuir−Hinshelwood HCOOH oxidation reaction mechanisms with two explicit water molecules from (a) **A1** and (b) **A2**. The lowest energy pathway is shown in red, while the next-lowest energy pathway is shown in blue. Individual ΔE values for intermediates (in bold) and activation barriers (in italics) are reported in eV. (c) Potential energy diagram comparing the two lowest reaction pathways.

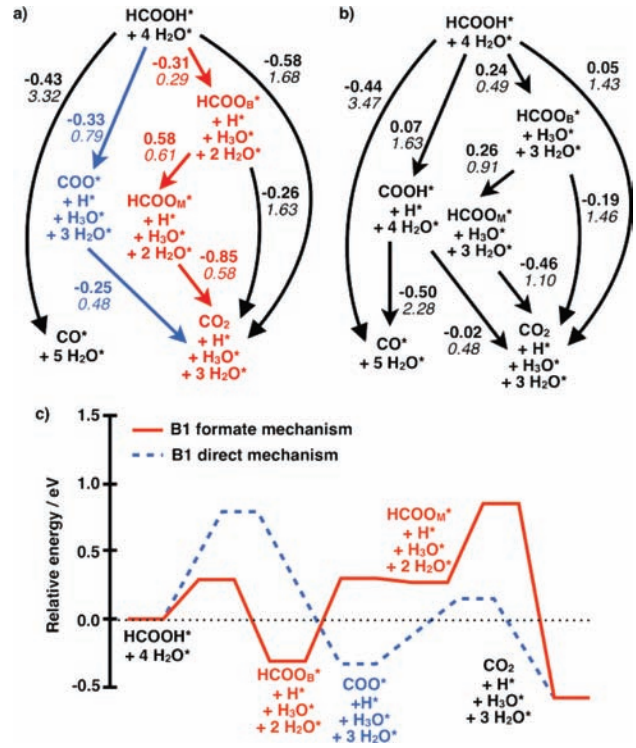

Figure 5. Langmuir−Hinshelwood HCOOH oxidation reaction mechanisms using the water bilayer solvation model starting from different orientations of HCOOH*: (a) **B1** and (b) **B2**. The lowest energy pathway is shown in red, while the next-lowest energy pathway is shown in blue. Individual ΔE values for intermediates (in bold) and activation barriers (in italics) are reported in eV. (c) Potential energy diagram comparing the two lowest reaction pathways.

are still in agreement with experiment, assuming the presence of CO* is related to defects or low-coordinated surface sites. Given the high barriers to CO* formation, we did not calculate further oxidations to CO_2*, though this topic has been studied with DFT in previous works.[38,39]

Summary of LH Mechanisms. After calculating these various reaction pathways, a more-complete picture of the HCOOH oxidation mechanism is possible. Using solvation model **A**, the minimum energy pathway (MEP) corresponds to the formate reaction pathways using models **A1** and **A2**. The calculated values are summarized in Figure 4. In both cases, the highest reaction barrier process is C−H activation from the $HCOO_M$* intermediate. In model **A1**, the barrier is 1.12 eV, while in model **A2** it is 1.18 eV. With solvation model **A**, one finds no reason to expect that a direct pathway would ever be competitive during a reaction process. This is of course problematic since HCOOH oxidation most likely operated via a dual-pathway mechanism.

Using solvation model **B**, the MEP is again the formate pathway; however, the next lowest energy process is the direct pathway involving the COOH* intermediate. Both of these pathways were found using model **B1**, and a summary of these data are presented in Figure 5. Using the bilayer model, the presence of a dual-pathway mechanism is at least more possible.

Simulating ER Mechanisms. Until now, our discussion of HCOOH oxidation has assumed that H atoms removed from HCOOH during oxidation remain at the electrochemical interface, either as a hydronium molecule or as an explicitly bound H* species. Instead, we can assume that each hydrogen atom removed from HCOOH* enters the electrolyte as a proton. Since the proton is removed into the bulk electrolyte, this would be an ER mechanism rather than an LH mechanism. Such ER mechanisms have been observed to be preferred in electrocatalytic oxygen reduction on Pt(111).[31] If one then assumes the proton immediately participates in the hydrogen electrode reaction shown in eq 2, it is then a coupled proton−electron-transfer process (CPET), and one can use this coupling to implicitly model applied electrode potentials (vs the RHE) via explicit shifts of calculated Fermi energies for different intermediates.[40] In other words, for every transferred H atom, the energy of the intermediate following this transfer is shifted by the desired electrode potential. Potential-dependent reaction barriers for these processes can also be approximated with an extension to this model, and further details of this approach can be found in refs 31 and 41.

$$H^+_{(aq)} + e^- \rightarrow {}^1/_2H_{2(g)} \qquad (2)$$

Previous DFT studies on the electrocatalytic HCOOH oxidation using different models found that an applied potential has little effect on oxidation barriers.[22,26] However, we have already shown that the bilayer solvation model sometimes substantially influences reaction barriers and intermediates, and so we now report ER mechanisms calculated within the bilayer models (Figure 6).

(38) Alavi, A.; Hu, P.; Deutsch, T.; Silvestrelli, P. L.; Hutter, J. *Phys. Rev. Lett.* **1998**, *80*, 3650–3653.
(39) Desai, S.; Neurock, M. *Electrochim. Acta* **2003**, *48*, 3759–3773.
(40) Bockris, J. O.; Reddy, A. K. In *Modern Electrochemistry 2B: Electrodiscs in Chemistry, Engineering, Biology and Environmental Science*; Kluwer Academic/Plenum Publishers: New York, 2001; pp 1539−1550.
(41) Keith, J. A.; Jacob, T. *Angew. Chem., Int. Ed.* 2010DOI:10.1002/anie.201004794.

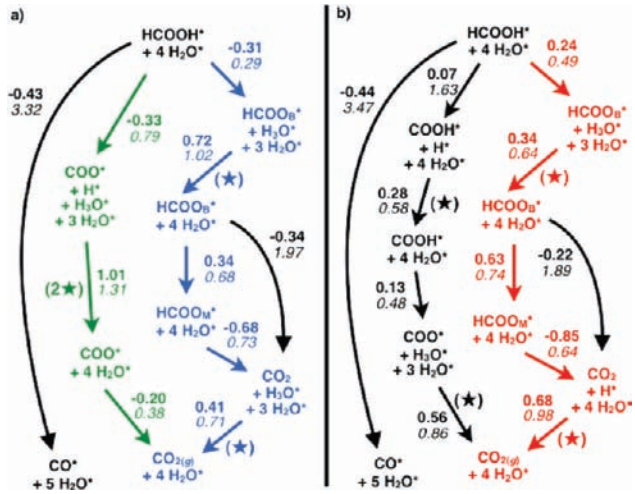

Figure 6. Eley−Rideal HCOOH oxidation reaction mechanisms with the water bilayer solvation model starting from different orientations of HCOOH*: (a) **B1** and (b) **B2**. The lowest energy pathway is shown in red, the next-lowest energy pathway is shown in blue, while the third-lowest energy pathway is in green. Reaction steps marked with a star (★) denote a coupled proton−electron-transfer (CPET) process between the interface and the electrolyte. Although the pathway denoted in (b) has the lowest individual barrier by 0.04 eV, its final product state is overall 0.56 eV thermodynamically less stable than the product states in (a). Therefore, only pathways in (a) are considered further.

The ER pathways involving CO formation are the same as the LH pathways because dehydrogenation leads to a fifth water molecule per (3×3) surface unit cell and no charge is transferred during CO oxidation. Thus, the reaction barriers for these processes remain very high ($E_{act} > 3.32$ eV), and this result remains in good agreement with electrochemical experiments.[14,15,19−21,37] ER pathways involving CO_2 formation do change because intermediates formed from a CPET no longer involve an explicit proton within the simulation cell. In general, all of the CO_2 pathways in both **B1** and **B2** models become thermodynamically more favorable as applied potentials increase, consistent with the general trends found by Neurock et al.[22] Figure 6 shows that the final product obtained using the **B2** model is 0.56 eV higher than the product found in the **B1** model. Since the relative energies of the final products are all influenced by the applied potential equally, we have to consider the potential dependence on the barriers for all of these processes.

We now report individual reaction processes including transition states at different applied potentials (Figure 7). At 0.0 V (vs the RHE), the MEP is the formate pathway in the **B2** model: $E_{act} = 0.98$ eV and $\Delta E = 1.04$ eV, overall. The highest barrier process for this mechanism is the potential-dependent CPET process removing H*. The next-lowest energy mechanism is the formate pathway in the **B1** model: $E_{act} = 1.02$ eV and $\Delta E = 0.60$ eV, overall, with respect to the more stable HCOOH* structure calculated in model **B2**. The highest barrier process for this mechanism is the CPET process after formation of the $HCOO_B$* intermediate. Lastly, the third-lowest energy pathway is the direct pathway in the **B1** model: $E_{act} = 1.31$ eV, and its final product is also 0.6 eV endothermic overall. Here, the highest barrier process is removal of two hydrogen atoms after formation of the CO_2* intermediate, a double-CPET process.

Although the formate pathway from **B2** model is calculated to have the lowest barrier of all, it is only slightly lower than the barrier for the formate pathway from the **B1** model. Both formate pathways should be considered competitive, but the **B1** pathway is more relevant, as it leads directly to a lower-energy final product structure. For now, we show both the formate and the direct pathways via the CO_2* intermediate as calculated in the **B1** model in Figure 7. Comparing the steps with the highest barrier in both mechanisms shows that, at low electrode potentials (0.0 V vs RHE), the formate pathway is strongly preferred on Pt(111) terraces over the direct pathway due to the high barrier associated with the high-energy double-CPET process in the latter mechanism.

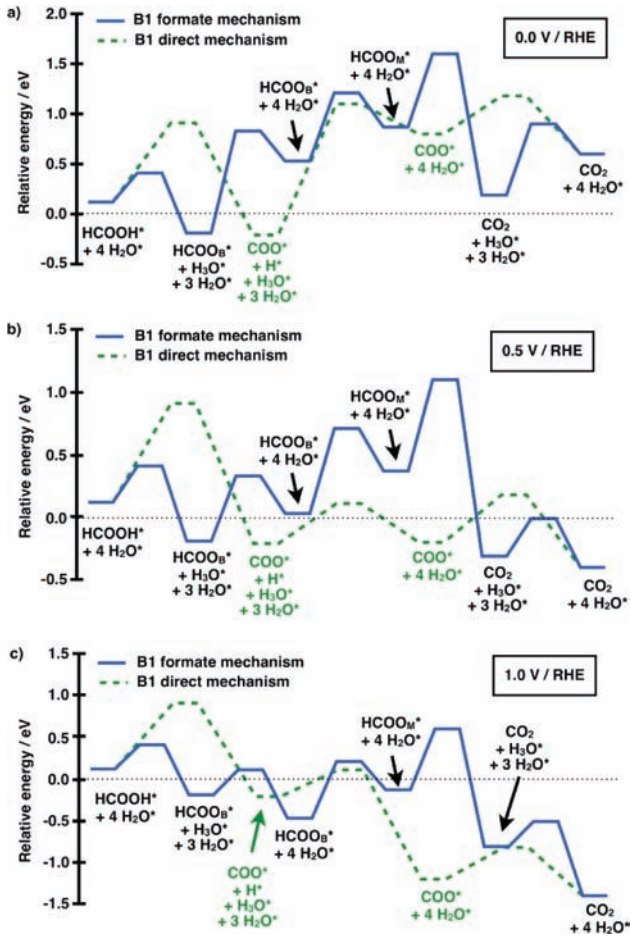

Figure 7. Comparison of Eley−Rideal HCOOH oxidation reaction mechanisms with the water bilayer solvation model at different applied potentials (vs the RHE). $U =$ (a) 0.0, (b) 0.5, and (c) 1.0 V.

At 0.5 V, the relative energies between the two **B1** pathways change, since the formate pathway has two separate CPET processes (after $HCOO_B$* and CO_2 formation), while the direct pathway has a double-CPET process (after CO_2* formation). The highest barrier in the formate pathway is now $E_{act} = 0.73$ eV ($HCOO_M \rightarrow CO_2$), while the highest barrier in the direct pathway is 0.79 eV (simultaneous C−H and O−H bond-breaking). Note that the highest barrier processes at 0.5 V are now potential-independent processes. Overall, the energy of the CO_2 final intermediate has decreased to −0.4 eV with respect to the most stable HCOOH* structure found in model **B2**. Overall, the difference between the formate and the direct pathways has decreased substantially with increased applied potentials. Instead of the highest barriers being different from each other by ∼0.3 eV at 0.0 V, the difference in barriers at 0.5 V is now only 0.06 eV.

At 1.0 V, the final product energies become even more stable due to the effect of the electrode potential on the final CO_2

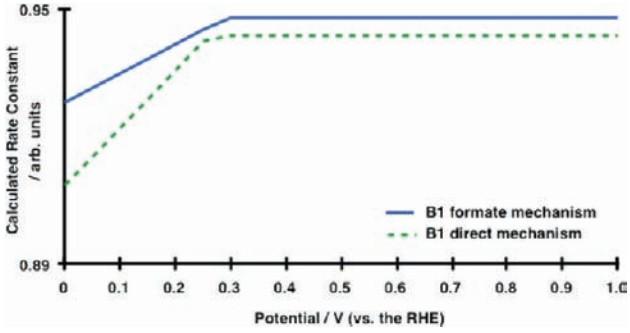

Figure 8. Comparison of potential-dependent rate constants as calculated from canonical transition-state theory. While the formate mechanism always has a larger calculated single rate constant than the direct pathway, both mechanisms appear to converge at potentials >0.2 V, implying that both mechanisms should be operational. At potentials <0.2 V, the formate pathway would ideally predominate on a Pt(111) terrace.

product state (−1.4 eV overall). Nevertheless, at 0.5 V the highest barrier in both the formate and the direct pathways were potential-independent processes, and those too are still in play at 1.0 V. Thus, the difference in barriers for the formate and direct pathways is again <0.1 eV.

Naturally, formic acid oxidation is a highly complicated process. Undertaking a kinetics analysis using rate constants derived from first-principles calculations would be an ideal way to determine which pathways are relevant under different concentrations of intermediates. Such a kinetics analysis is unfortunately difficult, since it would require coverage dependencies and reaction processes at step-edges and defect sites to provide a realistic modeling of the real electrochemical system. However, our calculations can be incorporated into a reduced kinetic model that should report *qualitative* features of the reaction mechanisms at different applied potentials. We do this by comparing calculated potential-dependent rate constants obtained from Eyring's canonical transition-state theory (TST),[42] as shown in eq 3:

$$k(U) = \frac{k_B T}{h} \exp\left(\frac{-\Delta^{\ddagger} G_T(U)}{k_B T}\right) \qquad (3)$$

where k_B is Boltzmann's constant, T is temperature, h is Planck's constant, and $\Delta G_T(U)$ is the highest barrier for a given mechanism at a given potential. Figure 8 shows a comparison between the potential-dependent rate constants for the formate and direct pathways in a potential range between 0.0 and 1.0 V.

As a first approximation, if one assumes that all intermediate concentrations are unity, Figure 8 would then correspond to the relative preference of the two HCOOH oxidation pathways at different potentials. At potentials <0.3 V, the formate pathway should be preferred over the direct pathway; however, it is not clear the degree to which this would be expected, since this is the region in which Pt(111) surfaces in HCOOH oxidation are largely covered with CO*.

Recall that the highest barrier process in the formate pathway is first the CPET process after $HCOO_B$* formation, but with increasing potential the highest barrier process changes to the $HCOO_M \rightarrow CO_2$ process. Based on the relative energies of the possible intermediates, $HCOO_B$ should be observable in electrochemical conditions, and indeed it is.[14,15,19,20] Furthermore, at potentials where the $HCOO_M \rightarrow CO_2$ process has the highest barrier, formate intermediates should accumulate on the surface. On the basis of our results alone, one would expect the $HCOO_M \rightarrow CO_2$ process to be slow at potentials ∼0.3 V and higher. Indeed, experiments have found that a formate adlayer starts to accumulate in the potential ranges >0.2 V.[20]

At potentials >0.3 V, our calculations show the two pathways converge toward very similar values suggesting that both pathways should be largely indistinguishable at potentials higher than 0.3 V. As the highest reaction barriers decrease when increasing the electrode potential from 0.0 to 0.3V, the rates for HCOOH oxidation should increase. Indeed, experimental Faradaic currents increase with increasing potential in the range of 0.1−0.7 V.[14,15,20] It has been rationalized that, at potentials >0.7 V, the surface is poisoned by oxide species, and hence a decrease in current activity should result. Since our calculations have not investigated HCOOH oxidation on Pt-oxide surfaces, there is no reason to think that hypothesis is unreasonable.

In our calculations, we considered the influence of solvation by adding different amounts of explicit water molecules to the system. Although the water movements as well as entropic effects introduced by the solvent are not included, we believe the present representation already provides important insights into the influence of electrochemical conditions. Certainly, suitable molecular dynamics (MD) studies, that would allow for using thermodynamic integration techniques, metadynamics, etc., would help to understand the role of these additional effects in reaction energies and activation barriers. Although in some cases these effects might become important, unfortunately widely usable MD techniques still have difficulties in separating electrostatic from non-electrostatic contributions to the free energy of solvation as well as reducing uncertainties in the molecular mechanics representation of the solvent.[43]

Importantly, we find that solvation changes the dominant pathway for HCOOH oxidation from strictly the formate pathway in gas phase[25] via the $HCOO_B$ intermediate to a dual-pathway mechanism involving both the same formate pathway and the direct pathway, with a highly transient CO_2* intermediate in electrochemical condition. The theoretically based observation in the gas phase is fully consistent with experimental results in ultrahigh vacuum,[44,45] while our results in electrochemical conditions provide a more fundamental understanding of this process at electrochemical interfaces to better explain corresponding experiments.[14,15,19−21] However, it should be mentioned that most experiments use rather rough surfaces, which should be kept in mind when comparing theory and experiment.

We note that the conclusions made herein differ slightly from early works by Neurock et al.[22] and Wang and Liu,[26] who both proposed that the dominant pathway is based on either the COOH* intermediate or a weakly adsorbed HCOOH* with the C−H bond in a configuration, a structure we found to be ∼0.6 eV less favorable than other HCOOH* structures. In contrast, we found the formate pathway to always be preferred over the direct pathway on clean surfaces, but at potentials >0.3 V, this difference is only ∼0.1 eV. Such a small energy difference (combined with the calculation inaccuracies) makes it difficult

(42) Eyring, H. *J. Chem. Phys.* **1935**, *3*, 107–115.
(43) Marenich, A. V.; Cramer, C. J.; Truhlar, D. G. *J. Chem. Theory Comput.* **2008**, *4*, 877–887.
(44) Columbia, M. R.; Crabtree, A. M.; Thiel, P. A. *J. Am. Chem. Soc.* **1992**, *114*, 1231–1237.
(45) Columbia, M.; Thiel, P. *Surf. Sci.* **1990**, *235*, 53–59.

to draw conclusions on the predominant pathway under electrochemical condition.

Conclusions

The Pt(111)-catalyzed HCOOH oxidation mechanism has been studied in electrochemical conditions, including the effects from the aqueous phase and an electrode potential. In a previous work where we investigated the reaction mechanism in gas-phase conditions, we found that HCOOH oxidation occurs via a single mechanism, the *formate pathway*. In contrast, the present study shows that electrochemical oxidation of HCOOH on platinum proceeds via a *dual-path mechanism* involving a *formate pathway* via the $HCOO_B$* intermediate and a *direct pathway* from HCOOH* via a highly transient CO_2* intermediate. When calculated on idealized terraced surfaces, these two pathways are nearly identical in energy; however, the contribution of the formate pathway may become larger with increasing potential because the coverage of formate increases and available sites for the direct pathway become reduced. In addition, the presence of other electrochemical species (CO_{ad}, OH_{ad}, or acid radical) may be also important for the above pathways. Since such co-adsorbates might additionally influence the reaction mechanism, future work will aim toward a detailed and comprehensive study of these effects, for which the present work provides an important basis.

From a methodological view, we show how the presence of solvation, particularly when modeled as a water bilayer, affects different reaction pathways compared to explicit solvation models containing few water molecules. Lastly, we show how electrode potentials can alter key reaction barriers, which in turn cause a particular pathway to become more favored at different potentials. The models we employed as well as the corresponding analysis may be used to describe other electrocatalytic reactions at electrochemical interfaces, making it an important tool for elucidating other electrocatalytic reactions.

Acknowledgment. The authors gratefully acknowledge support by the "Deutsche Forschungsgemeinschaft" (DFG) and the Alexander von Humboldt foundation (AvH), as well as the bw-grid for computing resources.[46] Further, support by the European Union through the Marie-Curie Initial Training Network ELCAT, Proposal No. 214936-2, 2008-2012, is acknowledged.

Note Added after ASAP Publication. Table 1 contained typographical errors in the version published November 30, 2010; the correct version reposted December 2, 2010.

JA1083317

(46) bwGRiD (http://www.bw-grid.de), a member of the German D-Grid initiative, is funded by the Ministry for Education and Research (Bundesministerium für Bildung und Forschung) and the Ministry for Science, Research and Arts Baden-Württemberg (Ministerium fuer Wissenschaft, Forschung und Kunst Baden-Württemberg).